CONF-9607139--1
UCRL-JC-124315
PREPRINT

SPENT FUEL CHARACTERISTICS & DISPOSAL CONSIDERATIONS

V. M. Oversby

This paper was prepared for submittal to
NATO Advanced Study Institute on Actinides and the Environment
Crete, Greece, July 7–19, 1996

June 1996

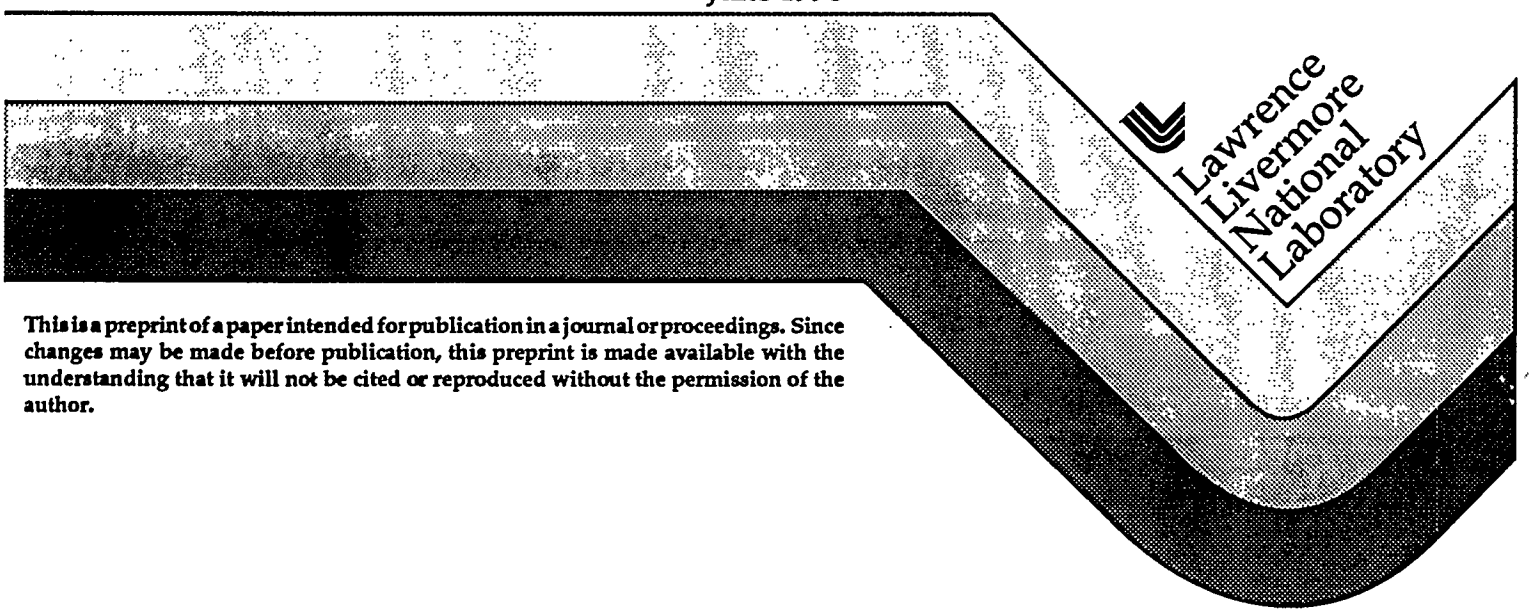

RB

DISCLAIMER

DISCLAIMER

SPENT FUEL CHARACTERISTICS & DISPOSAL CONSIDERATIONS

V. M. OVERSBY
LAWRENCE LIVERMORE NATIONAL LABORATORY
LIVERMORE, CA 94550

1. Introduction

The fuel used in commercial nuclear power reactors is uranium, generally in the form of an oxide. The gas-cooled reactors developed in England use metallic uranium enclosed in a thin layer of Magnox. Since this fuel must be processed into a more stable form before disposal, we will not consider the characteristics of the Magnox spent fuel. The vast majority of the remaining power reactors in the world use uranium dioxide pellets in Zircaloy cladding as the fuel material.

Reactors that are fueled with uranium dioxide generally use water as the moderator. If ordinary water is used, the reactors are called Light Water Reactors (LWR), while if water enriched in the deuterium isotope of hydrogen is used, the reactors are called Heavy Water reactors. The LWRs can be either pressurized reactors (PWR) or boiling water reactors (BWR). Both of these reactor types use uranium that has been enriched in the 235 isotope to about 3.5 to 4% total abundance. There may be minor differences in the details of the spent fuel characteristics for PWRs and BWRs, but for simplicity we will not consider these second-order effects.

The Canadian designed reactor (CANDU) that is moderated by heavy water uses natural uranium without enrichment of the 235 isotope as the fuel. These reactors run at higher linear power density than LWRs and produce spent fuel with lower total burn-up than LWRs. Where these difference are important with respect to spent fuel management, we will discuss them. Otherwise, we will concentrate on spent fuel from LWRs.

2. Fuel chemical composition

2.1 FRESH FUEL

Light water reactor fuels are made from uranium that has been enriched in ^{235}U from the natural abundance of 0.7% up to 3 to 4%. Uranium dioxide powder is cold-pressed into pellets, which are sintered at high temperatures to produce a product that is 95% of theoretical density and is fine-grained, with average grain size of a few μm. The pellets are about 1 cm in diameter and 1 to 1.5 cm high and are packed into thin-walled tubes of Zircaloy, an

alloy consisting predominantly of Zr with 1.6% Sn [1, 2]. The fuel is very close to stoichiometric UO_2 at the time of manufacture [3]. If there is any excess oxygen in the fuel, it will be taken up by the Zircaloy cladding as soon as the fuel is used in the reactor.

Fuel pins are mounted into arrays to become the fuel assemblies inserted into the reactor core. For BWRs, the array size is approximately 8 x 8, while for PWRs the size is approximately 16 x 16. The assembly structural materials are Zircaloy, Inconel X-750, and stainless steel (302 and 304) for BWRs and Inconel 718, stainless steel (302 and 304), and Nicrobraze 50 (a NiCrP alloy) for PWRs [2].

2.2 IRRADIATED FUEL

2.2.1 *Fission Products*

During irradiation in the nuclear power reactor, the energy content of the fissile isotopes in the fuel is converted into heat and then into electric power. Initially, for LWR fuels, the only fissile isotope is ^{235}U; with time, the ^{238}U captures neutrons and the product nucleus decays to fissile ^{239}Pu. For fuel with normal levels of burn-up the fission products are produced from both fissile ^{235}U and ^{239}Pu. Each fission reaction produces two major fission products and, on average, 2.1 neutrons. The mass distribution for fission products produced by thermal-neutron induced fission is slightly different for each parent isotope. Since the proportion of fission products due to ^{239}Pu fission increases as burn-up increases, the distribution of total fission products changes with burn-up. A computer model, ORIGEN2, can be used to calculate the chemical composition of reactor fuel as a function of burn-up and time since the fuel was removed from the reactor. The latter parameter is important because the fuel chemistry changes as radioactive isotopes of one element are transmuted into stable isotopes of the same element or a different element.

Table 1 gives the results of an ORIGEN2 calculation for spent PWR fuel with a burnup of 35 megawatt days per kilogram of heavy metal (MWd/kgM) at a time of 6 years after removal from the reactor. The composition is given as chemical element totals, grouped so that elements with similar chemical behavior are together. All elements that represent more than 1 mg/kg (or ppm) in the spent fuel are listed. While 32 chemical elements are present in the list of significant fission products, the distribution is dominated by a small group of elements. The rare gases account for 16.7% of the fission product mass, while Y + the rare earth elements account for 29.7%.

Kleykamp [5] proposed a four-fold classification of fission products based on their expected chemical behavior in spent fuel. The rare gases and the minor amounts of halogen elements would be expected to segregate from the fuel matrix. Mo plus the noble metal fission products account for 24.7% of the fission products; these elements, as well as Ag, Cd, In, Sn, Sb, and Te would be expected to be in the metallic state in spent fuel. Elements that are expected to form separated oxide phases are Rb, Cs, Ba, and Nb (which is present as less than 1 ppm in the fuel, so is not included in Table

1). The rare earth elements and Sr are expected to exist in solid solution with the uranium dioxide. Zirconium, which accounts for 10.1% of the fission product mass, can form a solid solution with the uranium dioxide matrix or could form a separated oxide phase. Mo and Te, which are expected to be in the metallic state, might also form oxides in the spent fuel.

TABLE 1: Calculated fission product yield for PWR fuel with burnup of 35 MWd/kgM in mg/kg of U at 6 yrs out of reactor [adapted from data in 4]. Only elements which represent more than 1 ppm are shown.

Chemical element	Concentration	Chemical element	Concentration
Krypton	359.9	Zirconium	3639.4
Xenon	5656.5	Yttrium	448.7
Bromine	22.1	Lanthanum	1269.0
Iodine	258.7	Cerium	2469.3
Rubidium	346.0	Praseodymium	1161.0
Cesium	2605.3	Neodymium	4189.8
Strontium	794.2	Promethium	25.8
Barium	1740.6	Samarium	815.2
Selenium	57.7	Europium	154.5
Tellurium	528.6	Gadolinium	141.5
Antimony	24.0	Terbium	3.2
Silver	91.8	Dysprosium	1.8
Cadmium	138.3	Molybdenum	3497.5
Tin	103.5	Technetium	798.8
Indium	2.4	Ruthenium	2404.9
		Rhodium	483.5
Subtotals	Col. 1	Palladium	1684.0
Rare gases	6016.4		
Halides	280.8	Subtotals	Col. 2
Alkalis	2951.3	Zirconium	3639.4
Alkaline Earth	2534.8	Y + REE	10680
Others	946.3	Mo + noble metals	8868.7
Total fission products shown		35917.5 ppm	
Total not shown		2.5 ppm	

2.2.2 *Actinide elements*

As fuel is irradiated in the reactor, the ^{238}U present absorbs neutrons, leading to the production after decay of the short-lived daughter products (^{239}U and ^{239}Np) of fissile ^{239}Pu. In addition to fission reactions, ^{239}Pu

can capture neutrons leading to the production of other actinide isotopes. Each of the isotopes produced is radioactive and is subject to decay during and after irradiation. In addition, each of the isotopes produced is capable of capturing a neutron leading to production of isotopes with higher mass. If the neutron capture cross sections and the decay constants are known, together with an accurate description of the reactor neutron spectrum, the final composition of actinide elements in the spent fuel can be calculated using ORIGEN2. Table 2 shows the result of such a calculation for the same conditions as used for Table 1 fission products. Only isotopes that are present at abundances greater than 1 ppm are shown.

Table 2: Actinide inventory by isotope at burnup of 35 MWd/kgM at 6 years out of reactor, in units of mg/kg (ppm).

Element	Isotope	Amount
Uranium	234	135.1
	235	5247
	236	3528
	238	9.446E+5
Neptunium	237	468.0
Plutonium	238	185.0
	239	5095
	240	2521
	241	1039
	242	619.5
Americium	241	393.5
	242m	1.1
	243	138.8
Curium	244	37.3
	245	1.9

3. Fuel assembly characteristics

Fuel for LWRs is arranged into fuel assemblies that provide for control of the reactivity of the fuel during irradiation. Both the fuel cladding and the assembly materials are chosen for their chemical and mechanical stability under reactor operating conditions and for their neutronic properties. It is very important to economic operation of the power reactor that the cladding and assembly components absorb as few neutrons as possible. It is not possible, however, to limit neutron absorption by these components to zero. Some of the product nuclei from cladding or structural components may be

stable isotopes (i. e., not radioactive); others will be radioactive and are called activation products because their radioactivity was "activated" by absorbing a neutron. Table 3 gives a physical description of typical BWR and PWR fuel assemblies.

Table 3: Physical characteristics of LWR fuel assemblies [after 2]

Parameter	BWR	PWR
Assembly length, m	4.470	4.059
Cross section, cm	13.9 x 13.9	21.4 x 21.4
Fuel rod length, m	4.064	3.851
Active fuel height, m	3.759	3.658
Fuel rod OD, cm	1.252	0.950
Fuel rod array	8 x 8	17 x 17
Fuel rods per assembly	63	264
Assembly total weight, kg	319.9	657.9
Uranium/assembly, kg	183.3	461.4
UO_2/assembly, kg	208.0	523.4
Zircaloy/assembly, kg	103.3[a]	108.4[b]
Hardware/assembly, kg	8.6[c]	26.1[d]
Nominal volume/assembly, m^3	0.0864	0.186

[a]Includes Zircaloy fuel-rod spacers and fuel channel
[b]Includes Zircaloy control-rod guide thimbles
[c]Includes stainless steel tie-plates, Inconel springs, and plenum springs
[d]Includes stainless steel nozzles and Inconel-718 grids.

The reason for concerning ourselves with the assembly size and components is that after irradiation in the reactor these materials will also need to be treated as waste materials or recycled into another use. Regardless of which approach is taken, the radioactivity of the materials as a result of activation reactions will be important. If direct disposal of intact spent fuel assemblies is the chosen closure of the fuel cycle, then the activation products in cladding and assembly components, the fission products, and actinides together constitute the radioactive inventory of the high level waste repository. If some form of reprocessing of spent fuel is conducted, then the three inventory components (cladding, assembly components, and fission products plus actinides from the fuel) may have separate disposal options. Since the cladding material and the assembly components may be disposed of by different means, we should note that for

Table 4: Radiological report in Curies for Zircaloy-2 irradiated in a BWR for 27.5 MWd/kgM fuel burnup. Activity per kg at 15 years after discharge [6, 7].

Isotope	Half-life	Curies
^{14}C	5730 y	1.50×10^{-3}
^{55}Fe	2.7 y	0.0126
^{60}Co	5.27 y	0.136
^{59}Ni	7.5×10^{4} y	2.28×10^{-4}
^{63}Ni	100 y	0.0312
^{90}Sr	28.8 y	3.18×10^{-6}
^{90}Y	64.1 hr	3.18×10^{-6}
^{93}Zr	$1.5 \times 10^{\wedge}$ y	5.92×10^{-4}
^{93m}Nb	13.6 y	3.24×10^{-4}
^{94}Nb	2.0×10^{4} y	1.77×10^{-4}
^{99}Tc	2.14×10^{5} y	1.70×10^{-8}
^{121m}Sn	55 y	2.01×10^{-3}
^{125}Sb	2.7 y	0.138
^{125m}Te	58 d	0.0336

Table 5: Radiological report in Curies for 304 stainless steel and Inconel-718 irradiated in a BWR for 27.5 MWd/kgM fuel burnup. Activity per kg at 15 years after discharge [6, 7].

Isotope	304 ss, Ci	Inconel-718, Ci
^{10}Be (1.6 my)	2.30×10^{-9}	1.15×10^{-9}
^{14}C	0.0244	0.0244
^{36}Cl (0.3 my)	9.06×10^{-9}	–
^{55}Fe	5.699	1.712
^{60}Co	10.94	63.94
^{59}Ni	0.0406	0.237
^{63}Ni	5.565	32.42
^{93}Zr	8.6×10^{-10}	4.2×10^{-7}
^{93m}Nb	4.7×10^{-10}	2.3×10^{-7}
^{94}Nb	2.12×10^{-4}	0.098
^{93}Mo (3×10^{3} y)	--	1.895×10^{-3}
^{99}Tc	--	3.59×10^{-4}

a PWR, most of the Zircaloy mass listed in Table 3 is cladding material, while for a BWR, about half of the Zircaloy is assembly components.
Table 4 gives the inventories calculated using ORIGEN2 of significant radionuclides in Zircaloy after irradiation, while Table 5 gives data for Stainless steel and Inconel. ORIGEN2 will overestimate the activation product activity for components that are not in the central fueled section of the assembly by a factor of 5 to 10 [8]; thus, the measured activities for stainless steel and Inconel components should be 5 to 10 times less than those given in Table 5. The activation product activities in all materials except Zircaloy-4, which is used as cladding material for PWR fuels, studied by Luksic were high enough to exceed the Class C level for low level waste established by the US Nuclear Regulatory Commission [8]. This means that the wastes cannot be disposed of as low level waste under US law. The amount of ^{94}Nb given in Table 4 for Zircaloy 2, which is the BWR cladding material, would also exceed the Class C low level waste limits of 0.2 Ci/m^3.

4. Fuel structure and segregation of fission products

4.1 GRAIN SIZE, CRACKING, AND GAS RELEASE

Uranium dioxide LWR fuels are fabricated to have small, uniform grain size, which may be as small as 2 to 4 μm [3] or as large as 18 to 20 μm [4]. The fuels for CANDU reactors typically are 5 to 10 μm grain size [3]. During reactor operation, the temperature at the centerline of the fuel pellets may be as low as 800°C or as high as 1700°C depending on the reactor type and on the linear heat generation rate of the fuel. Fission products can relocate in the fuel by diffusion. For temperatures up to 1000°C, diffusion is controlled by an athermal process related to radiation damage in the material that results in a root mean square diffusion distance of about 0.3 μm/yr [9]. For higher temperatures, the diffusion rate increases with temperature, producing an average diffusion distance of about 5 μm/yr for Xe at low concentrations. For LWRs, the fuel is irradiated at average linear power of 15 to 25 kW/m, giving a centerline temperature between 800 and 1200°C, while for CANDU reactors, the average linear power is up to 55 kW/m, with 35% of the fuel run with centerline temperatures above 1300°C [3]. The higher fuel temperatures for CANDU fuels lead to higher average fission gas segregation than for LWR fuels.

Another effect seen in fuels due to elevated temperature is grain growth, also called restructuring, which occurs by a process similar to sintering. Fission products that have limited solubility in the fuel matrix can be segregated to the grain boundaries during restructuring. Forsyth [10], measured the porosity and average grain size for a PWR fuel with average burnup of 43 MWd/kgU as a function of radial position in a fuel pellet. As we will discuss further below, the burnup in fuel is not uniform throughout

the pellet, but increases rather dramatically at the pellet rim. This increase in burnup is accompanied by an increase in porosity [11, 12]. Table 6 illustrates the modest increase in grain size at the pellet center as well as the increase in porosity at the pellet rim.

Table 6. Porosity and grain size of spent fuel as a function of radial position for PWR fuel with burnup of 43 MWd/kgU [data from 12].

Radial Position from center, mm	Total Porosity in percent	Average grain size, μm
4.0	3.4	4.3 ± 0.1
3.0	1.6	4.5 ± 0.1
2.0	0.75	not given
1.0	1.4	5.5 ± 0.1
0	1.5	5.7 ± 0.2

Spent fuel characterization has been undertaken for materials used in the Swedish and United States programs examining the leaching and dissolution behavior of fuels [10, 12, 13]. Normal operating conditions for LWRs lead to fission gas release from the fuel pellet to the gap between the pellet and cladding that is 1% or less. Occasionally, a fuel is found that shows high fission gas release. Guenther et al. [13] examined a fuel with 11.2% fission gas release, accompanied by clear evidence in gamma scans of redistribution of fissionogenic cesium. Examination of the cladding inner surface revealed accumulations of ^{137}Cs and ^{129}I. The fuel also showed substantial grain growth from an initial size of 7 μm to a final size of 16 μm. All of these findings point to the fuel rod having experienced a higher than normal operating temperature. Comparison of two fuel rods taken from the same BWR reactor showed a clear correlation of grain growth with fission gas release: 0.6% gas release accompanied by 10% grain growth and 8% gas release accompanied by 80% grain growth [13].

CANDU reactor fuels, which operate at a higher linear power than LWRs, typically show higher fission gas release than LWR fuels [3]. In addition, bubbles of gas accumulate on the grain boundaries in high gas release CANDU fuels. All uranium dioxide fuels have transgranular fracturing morphology before use and intergranular fracturing after normal irradiation. Segregation of gases, and possibly some other fission products that are volatile at reactor operating conditions, may be responsible for this weakening of the intergranular bonding.

LWR fuels show radial cracking patterns across the fuel pellets after irradiation [3, 11, 12]. These cracks form during reactor startup or

shutdown, when steep thermal gradients develop in the fuel pellets. These cracks do not seem to affect fission product segregation, but they do cause the fuel to fragment, which increases the surface area of the fuel. This could be important in the interpretation of leaching and dissolution testing of fuels [11]. Table 7 shows the size distribution for the reference fuels used in the Swedish program.

Table 7. Fuel fragment size distribution in fuels used in the Swedish fuel characterization program, wt % [12].

Size fraction	BWR fuel	PWR fuel
> 4mm	64.7	23.8
2-4 mm	31.1	68.7
1-2 mm	3.0	4.7
0.5-1 mm	0.8	1.9
<0.5 mm	0.4	1.0

4.2 NOBLE METAL PARTICLES

Studies of LWR fuels irradiated under high power conditions and of breeder reactor fuels provided information on materials that had operated under higher temperatures than for standard LWR fuels [5, 14]. The higher temperatures provided greater opportunity for fission product segregation, grain growth, and separated phase formation. It is possible that the phase relations for segregated materials are different at the higher temperatures than for materials exposed to normal operating conditions; however, the coarser grain size allowed separated phases to be studied in these fuels long before they were identified in normal LWR fuels.

Kleykamp [5] identified three phases containing noble metals in annular breeder fuels. They were Pd-Ag-Cd and Pd-Sn-Sb-Te ingots in the central void region formed by vapor transport, and a MoTcRuRhPd alloy. The detailed chemistry of the 5-metal alloy will depend on whether the fuel is an LWR fuel or a Pu-containing breeder fuel, since the fission yield for these metals is different for ^{235}U and ^{239}Pu. Also, as normal or slightly higher enriched LWR fuels are taken to higher burnup, more of the fission products in the final fuel will be produced from ^{239}Pu formed from ^{238}U during the irradiation process. Examination of a high burnup (4.3 atom %), high linear power rating (43 kW/m) LWR fuel by Kleykamp [14] showed the presence of 2 alloy phases, one with 52% Mo and 32% Ru, while the other had 27% Mo and 46% Ru.

Transmission electron microscope studies on LWR fuels irradiated under normal operating conditions were reported by Thomas and coworkers [15, 16]. These studies are difficult to perform because the radiation from the fuel interferes with the instrument detection system and produces a large background noise signal. This background signal is also a problem with analytical electron microprobe studies of spent fuel. Advances in specimen preparation methods to limit the sample size used in the measurements allowed the TEM studies to be successful.

Studies using Turkey Point spent fuel with 27 MWd/kgU burnup, 92% theoretical density at fabrication, <0.3% fission gas release, and grain size of 10 to 25 μm using classical ceramographic methods showed no evidence for grain growth, fission gas bubbles, fission product particles, or grain cracking. TEM examination, however, showed grain boundaries decorated with 10-20 nm particles and smaller gas bubbles [15]. Near the grain boundary there was a zone of 0.3 to 0.4 μm that was denuded of particles or bubbles, suggesting that diffusion from this region was the source for the material found on the grain boundaries and for the gas found in the pellet-cladding gap. Chemical analysis by Energy Dispersive Spectroscopy (EDS) gave a composition of 40Mo:30Ru:10Tc:15Pd:5Rh, which is similar to the expected fission yield of these elements. No other segregated fission products or actinide phases were found in this study. The metal alloy phase had the epsilon-Ru structure, as do the separated alloy phases in larger-sized particles found in fuels with higher temperature histories. Most of the fuel grains had 1 or 2 microcracks surrounded by dislocation tangles. The cracks were 1 to 2 μm long and were frequently decorated with gas bubbles and alloy particles.

Further studies of 2 PWR fuels and one BWR fuel with moderate burnup and low fission gas release showed fission gas bubbles and epsilon-Ru alloy particles both on the grain boundaries and in the interiors of grains [16]. The size of the particles increased from 1-8 nm particle/bubble pairs at the rim of the fuel pellet to 50-100 nm alloy/gas pairs in the highly strained fuel matrix in the center of the pellet. The composition of the alloy phase was the same as found in the Turkey Point fuel. The gas phase in the segregations near the center of the fuel had a density of 2 to 3 gm/cm^3, which is nearly that of a solid phase. Particles found on the grain boundaries in the central region were only the metal alloy phase. The gas that separated to the grain boundaries in this high temperature region of the fuel apparently escapes to the pellet-cladding gap. Thomas and Guenther [16] noted that the thermodynamic studies of Kleykamp [5, 17] predict 2 alloy phases should be found in spent fuel with moderate burnup - the epsilon-Ru phase and a ß-Ru phase - while the TEM studies could only identify one phase. Also, the other segregated phases found in breeder fuels and high temperature fuels could not be identified in the moderate burnup LWR fuels at the resolution of the TEM studies.

Several studies have examined the noble metal insoluble residues resulting from acid dissolution of spent LWR fuels [18, 19, 20]. Adachi et al. [18] dissolved moderate burnup LWR fuel in 3 M nitric acid for 2 hours at 100°C and found that noble metal particles accounted for 70% of the

insoluble residues. The particles has composition of 20Mo:50-60Ru:10Pd:0.5-5Tc:10Rh in comparison with the expected composition of 42Mo:25Ru:16Pd:10Tc:7Ru. The difference in composition of the residues from the expected composition was interpreted by the authors [18] to be due to Mo and Tc being in other locations in the fuel. Since Thomas et al. [15] found the expected composition for the metal alloy particles in fuel that was intact, Oversby [11] suggested that the difference in composition was due to preferential leaching of Mo and Tc under the oxidizing conditions of nitric acid dissolution. Forsyth [19] dissolved both BWR and PWR moderate burnup fuels in cold 6N nitric acid and recovered metal particles that represented 80 to 86 % of the insoluble residues. The residues represented about 0.5 % of the fuel, in comparison with the yield of noble metals shown in Table 1, which is 0.88 %. This suggests that some of the particles, such as the very small particles found in grain interiors, had dissolved, while the larger particles were only partially leached. The composition of the particles recovered was 19Mo:53Ru:10Tc:10Pd:7Rh. This shows similar Mo depletion in cold nitric acid as was found in hot acid, but less Tc leaching, perhaps indicating that conditions of dissolution were somewhat less oxidizing in cold acid.

4.3 THE RIM EFFECT

During irradiation of fuel, neutrons are absorbed by ^{238}U leading to production of ^{239}Pu in the fuel. This process occurs preferential at resonance energies for absorption, which in turn leads to most capture occurring in the rim of the fuel pellet, as well as a lower neutron flux in the center of the fuel pellet. The ^{239}Pu can either fission or capture a neutron, leading to a build up of excess fission products and higher actinides in the pellet rim. This process becomes increasingly important with fuel burnup and is accompanied by an increase in porosity of the fuel rim material. For fuel with an average burnup of 45 MWd/kgU Matzke et al. [21] found a zone of increased porosity at the rim that represented 9 % of the pellet volume. This high porosity zone increased to 17 % of the volume for an average burnup of 53 MWd/kgU. The distribution of Cs, Pu, and Xe in the fuel was measured using electron microprobe analysis. Most of the build up in Pu and Cs occurred in the outer 100 μm of the pellet. Over this region there was a gradual decrease in fission Xe retained in the fuel as the surface of the pellet was approached. These results of these analyses are shown in Figure 1.

Forsyth [12] studied the rim effect in the Swedish PWR and BWR reference fuels, which were selected to represent average fuels destined for ultimate direct disposal in a high level waste repository. He found that the zone of increased porosity in the fuel was limited to about 30 to 40 microns from the pellet rim, with pores on the order of 1 μm in diameter. Forsyth [12] also examined samples from a BWR fuel rod with variable burnup along the pellet stack. The samples studied had average burnup of 21.2, 36.7, and 49.0 MWd/kgU. The highest burnup sample had a porous zone about 20 μm wide and showed poorly defined grain structure indicating

recrystallization of the original grains into a fine mosaic. The 36.7 MWd/kgU sample showed no porous rim zone and had grain structure at the rim that was typical of the original grain structure. Forsyth [12] noted that a porous rim zone of 50 μm represents about 2% of the pellet's volume and, because of the enhanced content of actinide there, would contain 3 to 4 % of the inventories of actinides and fission products. This is important in trying to interpret the significance of the small amounts of radioactive species released rapidly to solution in dissolution and leaching tests.

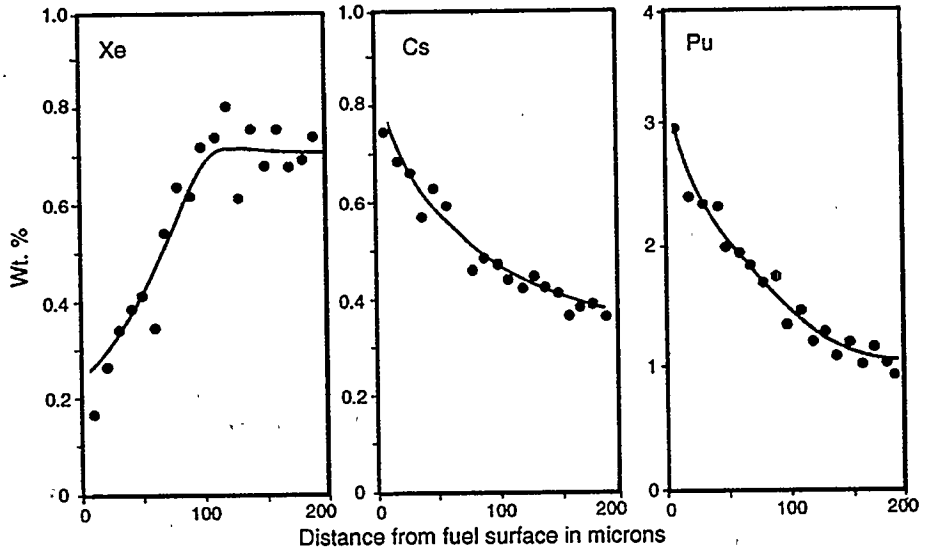

Figure 1 Concentration of Xe, Cs, and Pu in the porous zone at the fuel pellet rim at high burnup [21].

More detailed examination of the 49 MWd/kgU samples revealed that indications of grain restructuring could be seen as deep as 230 μm from the pellet surface. The local burnup at that depth is 53 MWd/kg in comparison with 66 MWd/kgU estimated local burnup at the pellet surface [12]. Near the pellet center, the only fuel restructuring seen was segregation of spherical particles of the 5-metal alloy phase.

Forsyth [12] also documented the local burnup across the pellets from the variable burnup rod and compared this to the variation in alpha activity across the pellets. The burnup varied from the low average value of 21.2 to a rim value of about 27 MWd/kgU, while for the highest burnup sample the average was 49 and the rim peak was 66 MWd/kgU, giving a total spread of a factor of 3.5. The alpha activity, however, showed a range from central values of 1 x 10^8 Bq/gU at the center of the 21.2 MWd/kgU sample to about 2 x 10^8 Bq/gU at that pellet edge, and 5 x 10^8 Bq/gU in the center of the 49

MWd/kgU sample compared with about 16 x 10^8 Bq/kgU at the pellet edge. Thus, the central alpha activity increased by a factor of 5 while the burnup increased by a factor of 2.5 and the rim activity increased by a factor of 8. The effect of these variations on the results of leaching and dissolution tests of these fuels is being investigated [12].

4.4 OTHER PHASES IDENTIFIED IN SPENT FUEL

Segregation of fission product phases occurs most readily in fuels that have operated at high temperatures. Kleykamp's studies of LWR fuels operated at high linear power ratings and of breeder fuels identified Cs_2MO_4, $Cs_2(U_{0.97}Pu_{0.03})_4O_{12}$, $(Ba,Sr)TeO_3$, BaO, Pu_2O_2Te, $Ba_{1-x}Sr_xO$, and $(Ba_{1-x-y}Sr_xCs_y)(U,Pu,Zr,Mo,RE)O_3$ in addition to the phase discussed above in relation to the noble metal alloys. Walker et al. [22] compared fuel with a normal (base) irradiation to 3 to 4 at.% at linear power between 30 and 18 kW/m to fuel that had transient testing to high linear power for 24 hours at 40 kW/m after the base irradiation. Two fission gas release episodes occurred during the base irradiation, one at 1 at.% burnup and the other at $2^1/2$ at.% burnup. Examination of the fuel after the base burnup showed that barium had migrated from the center of the pellet and had accumulated in a region about half way to the pellet edge. No segregated phases of barium could be identified in this sample, however. After the transient testing, segregated BaO and Ba-silicate phases were identified.

Cordfunke and Konings [23] calculated the expected speciation of some fission products in spent fuel based on their thermodynamic properties. They concluded that I should be present as CsI, Te as Cs_2Te, and the remainder of the Cs should be present as Cs_2MO_4 at oxygen potentials greater than -524 kJ/mol, a condition that should pertain to normal LWR fuels. Apart from the Cs_2MO_4 identified in fuels run at high temperatures, these phases have not been identified in LWR fuels.

5. Fuel Dissolution Tests

5.1 DISSOLUTION TESTING PROGRAMS

Countries that plan to dispose of spent LWR or CANDU reactor fuels directly - i.e., without chemical reprocessing to recover potentially useful materials - have studied the behavior of fuel samples when they are contacted with water. The three countries that have conducted the major part of these tests are Canada, Sweden, and the United States. The results obtained under programs conducted in these countries are reviewed in references 3, 11, 24, and 25. In this section, we will summarize the broad aspects of the results of dissolution tests. In general, the results from all three programs are in agreement. Where there are differences, they will be mentioned; otherwise, data from one program will be used to illustrate particular effects. The aqueous solutions used in these studies are deionized

water, dilute groundwaters (either natural or synthetic), or saline solutions to represent deep granitic groundwaters.

5.2 RAPID RELEASE FRACTION

When fuel is first put in contact with water, a fraction of the ^{137}Cs inventory that is comparable to the amount of fission gas released to the pellet cladding gap is found in the solutions. For CANDU fuels tested in solutions that contain KI carrier, the amount of ^{129}I released rapidly was similar to the amount of ^{137}Cs [26]. When tests were conducted in water that did not include the KI carrier, the release of ^{129}I was much less [27], suggesting that the ^{129}I is attached or sorbed on some interior surface of the fuel sample. Wilson [28] found ^{129}I release at 25°C from PWR fuel and cladding to dilute groundwater was two orders of magnitude less than ^{137}Cs release, but at 85°C, the difference in release was only 0.3 for I/Cs. He interpreted this to mean that the I was associated with the inner cladding surface from which it was only slowly released at the lower temperature. This would be consistent with the need to use KI carrier in the CANDU tests, since with abundant natural I in solution, ion exchange could release ^{129}I to solution from binding sites on the cladding.

5.3 MATRIX DISSOLUTION AND ALTERATION

Cesium and I have high solubilities in the solutions used in spent fuel dissolution and leaching tests. Most other elements in spent fuel have their concentrations in solution limited by solubility limits, which makes it very difficult to determine the rate at which the original UO_2 matrix is altering. Kleykamp [5] classified fission products according to their expected behavior in spent fuel. His four categories were

1. Fission gases and other volatile fission products - Kr, Xe, Br, I.
2. Fission products forming metallic precipitates - Mo, Tc, Ru, Rh, Pd, Ag, Cd, In, Sn, Sb, Te.
3. Fission products forming oxide precipitates - Rb, Cs, Ba, Zr, Nb, Mo, Te.
4. Fission products dissolved as oxides in the fuel matrix - Sr, Zr, Nb, REE.

We would also expect the transuranic elements to dissolve in the fuel matrix as oxides; however, because of their low solubilities in solutions with near-neutral pH, they could not be used to monitor fuel alteration rate. Reviewing the list of behavioral types above shows that the only promising candidate for a fission product with reasonably high solubility to act as a monitor of matrix dissolution is Sr [24].

Wilson [28, 11] reported the results of dissolution tests of spent PWR fuel in dilute bicarbonate ground water at 25°C and 85°C. In these tests, the concentrations of leached elements in solution were measured as well as the amount of elements recovered by rinsing the fuel after decanting the rinse solution. In addition, the leaching vessel was stripped using an acid solution

and the concentrations of materials recovered in the strip solution were measured. The sum of the dissolved, rinsed, and stripped materials was recorded as "total release". The tests were conducted under oxic conditions, but in sealed containers for the higher temperature tests, so the amount of oxygen available may have been limited. The total duration of the tests was about 15 months. Total U recovered at 25°C during the first 174 day cycle was 2 parts in 10^5 of the total inventory in the test, while the ^{90}Sr recovered was 40 parts in 10^5. At the higher temperature, about 9 parts in 10^5 of the uranium was recovered at the end of the first cycle, while the amount of ^{90}Sr recovered was still about 40 parts in 10^5. This can be interpreted in two ways. First, it may be that some of the ^{90}Sr is located in regions that are more accessible to leaching than the general matrix of the fuel. Alternatively, the uranium dioxide matrix may dissolve by oxidative dissolution, with U(IV) being oxidized to the more soluble U(VI) state, followed by precipitation of secondary phases onto the fuel surfaces. Since the amounts of expected precipitated phases are small, it would be extremely difficult to find them on the fuel after the tests.

Table 8: Total release of actinide, Tc, and Sr from PWR fuels into dilute bicarbonate groundwater. HRB = HR Robinson, TP = Turkey Point. Cycles lengths: cycle 1- 174d, cycle 2 - 181d, cycle 3 - 97d. [data from 28].

Element	Cycle	Fractional release - parts in 10^5 of inventory HBR-25°C	HBR-85°C	TP-85°C
Uranium	1	1.86	8.75	9.35
	2	1.24	3.1	1.3
	3	1.13	ND	0.9
Plutonium	1	4.0	10	6.0
	2	1.1	2.7	2.1
	3	1.2	ND	1.4
Americium	1	6.8	11.8	7.7
	2	1.5	3.3	2.2
	3	1.3	ND	1.5
Curium	1	10.1	16.1	9.2
	2	2.3	4.3	2.6
	3	1.7	ND	1.6
Technetium	1	25	12	89
	2	8	56	39
	3	<8	34	19
Strontium	1	41	41	43
	2	12.8	33	15.6
	3	7.5	6.2	8.6

Table 8 summarizes the data for total release of uranium, actinide elements, technetium and strontium for all three cycles of Wilson's tests[28]. For both fuels and for both temperatures the actinide release followed the pattern of Cm>Am>Pu; however, the differences in total release among the actinides were small for cycle 3 and they were approaching the uranium total release. For the first cycle of the 25°C test, 40% of the U and 33% of the Pu were recovered in solution samples, while 17% of the Am and 16% of the Cm were in solution samples. For the first cycle for HBR fuel at 85°C, 11% of the U, 10% of the Pu, and 5.5% each of the Am and Cm were in solution samples. The remainder of the material was recovered about equally in the rinse and acid strip fractions for Pu at 25°C, while Cm and Am at both temperatures were found predominantly in the acid strip, as was the Pu at 85°C. For the second and third cycles, uranium recovered in solution samples was about 15% at 25°C and 10% at 85°C, while Pu and the higher actinides were recovered only as a few perecent in solution at 25°C and as <0.05% at the higher temperature. These data strongly suggest that the formation of secondary phases will control the mobility of the actinide elements under direct disposal conditions, even under oxidizing conditions.

5.4 TECHNETIUM AND STRONTIUM RELEASE

In contrast to the behavior of the actinides, Tc was recovered 90% or more in solution samples with the exception of the first cycle HBR-85 sample where only 55% was recovered in solution. Strontium was recovered at 85 to 90% in solution at the lower temperature and only about 50% at the higher temperature. Strontium may be incorporated into carbonate phases, which may precipitate from the bicarbonate groundwater as the temperature is increased due to the lower solubility of $CaCO_3$ at the higher temperature.

While the amounts found in solution changed dramatically with temperature, it is interesting to note that the total release of U, the higher actinides and even Tc and Sr do not show a large difference between the two temperatures. Neither is there much difference in total release for the two fuels at the higher temperature. This is encouraging in that it suggests that bounding values on the rate of matrix degradation, which is what the total release parameter really is measuring, can be established.

Technetium occurs in the 5-metal alloy phase in the spent fuel and must be oxidized to dissolve. This may occur as preferential removal of Tc (and also Mo) from metal particles that are located on grain boundaries. An alternative mechanism for release is for the very small particles found inside the grains to dissolve completely as the fuel matrix is corroded. The release of Tc is greater than that of U by a factor of about 15 in the first cycle at 25°C; the difference reduced to a factor of about 6 for the later cycles. At the higher temperature, the data for first cycle HBR cannot be reliably used since it is suspected that oxygen may have been consumed inside the reaction vessel due to vessel corrosion and the conditions may have caused

precipitation of Tc. For the TP test, Tc release was 10 times that of U for the first cycle. For the later cycles, the Tc release exceeded U by a factor of 20 to 30. For both HBR and TP (when compared to previously published data for room temperature tests) the release of Tc increased substantially at the higher temperature. This contrasts with the behavior of Sr, which showed about the same total release at both temperatures. The Sr release began at about 20 times the U release at 25°C and decreased in subsequent cycles to 10 times and 7 times the U release. At the higher temperature, because more uranium was recoved in the acid strip solutions, the effective release ratio of Sr/U was less in the first cycle, but appeared to be about 10 for the later cycles.

5.5 SECONDARY PHASES

Wilson [28] recovered secondary uranium phases formed during the 85°C tests. The leaching solution contained about 30 ppm Si, which allowed uranium silicates to form. A needle-shaped crystalline phase was identified as uranophane - $CaO{\cdot}2UO_3{\cdot}2SiO_2{\cdot}6H_2O$ - and a phase with massive flake morphology was identified as haiweeite - $CaO{\cdot}2UO_3{\cdot}6SiO_2{\cdot}5H_2O$. There was some evidence in the x-ray diffraction data also for soddyite - $2UO_3{\cdot}SiO_2{\cdot}2H_2O$. Spent fuel that has been exposed to reactor cooling water during irradiation through a breach in the cladding has been shown to develop a surface alteration layer of the sub-monohydrate of schoepite, $UO_3{\cdot}xH_2O$, where x = 0.7 to 0.9 [29]. This phase or a closely related phase has also been identified on CANDU fuel tested in deionized water [30].

Forsyth et al. [31] conducted tests of PWR fuel segments in cladding exposed to dilute bicarbonate groundwater for two sequential exposures of 82d and 170d; two specimens were then given a long exposure of 436d with one sample in deionized water and one in dilute groundwater under ambient hot cell temperature. After termination of the experiments, the samples were examined visually and it was noted that the ends of the sample exposed to deionized water were covered with a yellow deposit, while the sample exposed to groundwater did not show this deposit. The samples were stored in their original Pt wire spiral holders in clean Pyrex beakers in the hot cell for about 5 months. During this time of exposure to air, the yellow deposit on the sample exposed to deionized water increased in size, but no deposit formed on the other sample. When the cladding was split open to examine the interior of the fuel segment it was found that the yellow deposit was limited to the ends of the specimen. This suggests that the environment inside the cladding is different from that seen by the exposed ends of the fuel. The deposit was determined by x-ray diffraction to be $UO_3{\cdot}0.8H_2O$ [31].

5.6 EFFECTS OF SPECIMEN GEOMETRY

Fuel tests in the Swedish program use short segments of fuel rods open at both ends. The fuel segments are held in spirals of Pt wire and suspended

in a leaching solution contained in a Pyrex beaker. All tests were conducted under ambient hot cell temperatures [24]. Tests conducted by Wilson at 25°C consisted of fuel fragments removed from a section of cladding. The fuel fragments and the cladding segment were both put into the leaching vessel; however the geometry of fuel/liquid contact is significantly different from that used in the Swedish tests. This appears to be the reason for differences in the total actinide release from the two different test programs.

The concentration of U in solution for tests conducted in contact with air at ambient temperature in dilute groundwater was found to be 4×10^{-6} mol/L in the Swedish tests and 6×10^{-6} mol/L in Wilson's tests conducted in fused silica vessels under similar conditions [24]. In Wilson's tests conducted in stainless steel vessels at ambient temperature, where the supply of air may have been limited because the vessels had a tighter fitting lid than the fused silica vessels, the concentration of U was 1.3×10^{-6} mol/L. These results are in rather good agreement. Concentrations of Pu in solution in the Swedish tests were 3×10^{-9} mol/L when all data were averaged and 8×10^{-10} mol/L when only exposures of over 200 days are considered. Wilsons's tests of HB Robinson fuel and Turkey Point fuel gave similar concentrations in solution [24].

The apparent paradox in the data is that the total release measurements for Wilson's tests show Pu total release to be greater that total U release, while the Swedish tests always have total Pu release much less than total U release under oxic conditions [24, 31]. The difference can be as large as a factor of 100 between U and Pu total release. In addition, in the Swedish tests with fuel segments, the rinsing and acid strip of the reaction vessels does not contain significant amounts of material, while for Wilson's tests with bare fuel, after the first reaction cycle, most of the released actinide material is found in the rinse and acid strip [11, 28]. In light of the observation discussed above concerning the location of secondary phase formation in the fuel segment test in deionized water, it seems that the explanation for the difference in total actinide release in the two test types may lie in the specimen geometry. If U is dissolved from the matrix and causes Pu to be mobilized, in Wilson's bare fuel tests the likelihood is that the Pu will precipitate onto the vessel walls. In the fuel segment tests, the mobilized Pu would still be inside the fuel segment and cladding; in this case it is likely that Pu would precipitate onto a fuel or cladding surface before it reached the bulk solution.

5.7 OXIDIZED FUEL

There are several ways in which the fuel matrix may become oxidized. This may happen during fuel storage prior to disposal if the fuel cladding contains a defect or is ruptured. Oxidation may also occur due to radiolysis effects in the fuel if the cladding is breached after disposal. For potential repository sites in the unsaturated zone (above the water table) there is air present in the rock pores, which can oxidize the fuel matrix over time. To determine the effects of oxidation on the dissolution of spent fuel, studies have been conducted on fuel samples that have been oxidized prior to

dissolution testing. Solution concentrations of U dissolved from fuels oxidized up to O/M (oxygen to metal ratio) of 2.33 were 20 ppm, about 10 times higher than the value found for testing fuel that had not been oxidized. Technetium release was also much higher from oxidized fuels [32].

5.8 BURNUP EFFECTS

Spent fuel that will be sent to a repository for disposal will have a range of burnups. As discussed above, the burnup affects the fission product distribution because of the component of fission coming from ^{239}Pu increasing in importance with higher burnup and because of the rim effect seen in fuels with relatively high burnup. To investigate the effects of burnup on dissolution properties of the fuel, Forsyth and Werme [24] used a stringer rod from Ringhals 1 reactor that had a large, smooth variation of burnup over the rod from 21.2 MWd/kgU at the bottom end of the rod to 49.0 MWd/kgU at the peak burnup position near the top of the rod. Specimens tested in dilute groundwater under oxic conditions (in contact with air) showed a gradual increase in the rapid release fraction of ^{137}Cs with burnup up to 32 MWd/kgU and a more rapid increase in release with burnup up to 40 MWd/kgU. At this point, the release remained constant with burnup from 40 MWd/kgU up to 46 MWd/kgU and then, surprisingly, decreased rather markedly as burnup increased to the peak value of 49 MWd/kgU. Strontium release showed a similar pattern. Since the fuel was irradiated in the same fuel rod, any variations in overall reactor performance can be ruled out as the cause of the unexpected result. It may, however, have something to do with Cs migration within the fuel rod during irradiation. To determine whether this effect is truly to be expected in bulk fuel from assemblies with higher burnup, further testing of such fuels would be needed.

6. Conclusions

Spent fuel characterization has shown that the original single phase uranium dioxide becomes a polyphase assemblage during irradiation. The elements of particular interest in assessment of the performance of a high level radioactive waste repository over long time scales are the actinides, especially Pu and U, Tc, Cs, I, and Sr if it can be used as an indicator of matrix degradation rate. Characterization of spent fuel has shown that some of the Cs and I in fuels segregates to the grain boundaries and/or the pellet/cladding gap during reactor operation and is available for rapid release as soon as the fuel is contacted by water. The amount of the rapid release fraction increases with burnup and with linear power at which the fuel is run. Thus, CANDU spent fuel has a high instant release fraction even though it has a low burnup. Tc is located in a 5-metal alloy phase in spent fuels. Stabilization in the alloy phase may help keep Tc immobilized even under mildly oxic conditions. More work is needed to determine the factors controlling long term behavior of Tc. Pu and U are released from the fuel at

approximately the same rate. Their ultimate fate is different since uranium forms secondary phases that do not seem to be the site of the Pu that precipitates from solution. Testing of fuel segments contained inside their original cladding gives Pu releases that are much lower than testing of bare fuels, suggesting that the cladding or the fuel pores may be the site of precipitation of the mobilized Pu.

X. References

1. Woodley, R. E. (1983) The characteristics of spent LWR fuel relevant to its storage in geologic repositories, Westinghouse Hanford Engeneering Development Laboratory report HEDL-TME 83-28, Richland, WA.
2. Roddy, J. W., Claiborne, H. C., Ashline, R. C., Johnson, P. J., and Rhyne, B. T. (1985) Physical and decay characteristics of commercial LWR spent fuel, Oak Ridge National Laboratory report ORNL/TM-9591/v1, Oak Ridge, TN.
3. Johnson, L. H. and Shoesmith, D. E. (1988), Spent Fuel, in W. Lutze and R. C. Ewing (eds.), *Radioactive Waste Forms for the Future*, North-Holland Physics Publishing, Amsterdam, pp. 635-698.
4. Guenther, R. J., Blahnik, D. E., Campbell, T. K., Jenquin, U. P., Mendel, J. E., Thomas, L. E., and Thornhill, C. K. (1988) Characterization of Spent Fuel Approved Test Material -- ATM-103, Pacific Northwest Laboratory Report PNL-5109-103, Battelle Pacific Northwest Laboratory, Richland, WA.
5. Kleykamp, H. (1985) The chemical state of the fission products in oxide fuels, *J. Nucl. Mater.*131, 221-246.
6. Friedlander, G., Kennedy, J. W., Macias, E. S., and Miller, J. M. (1981) *Nuclear and Radiochemistry, 3rd Edition*, John Wiley & Sons, New York.
7. Office of Civilian Radioactive Waste Management (1987) *Characteristics of Spent Fuel, High Level Waste, and Other Radioactive Wastes which may require long-term isolation, DOE/RW-0184 Vol. 1*, U. S. Department of Energy, Washington, DC.
8. Luksic, A. (1989) Spent Fuel Assembly Hardware: Characterization and 10 CFR 61 Classification for Waste Disposal, Pacific Northwest Laboratory Report PNL-6906 Vol. 1, Richland, WA.
9. Matzke, Hj., and Blank, H. (1989) *J. Nucl. Mater.* **166**, 120-131.
10. Forsyth, R. S. (1987) Fuel rod D97/B15 from Ringhals 2 PWR: Source material for corrosion/leach tests in groundwater; Final rod/pellet characterization program part one, SKB Technical Report 87-02, Stockholm.
11. Oversby, V. M. (1994) Nuclear Waste Materials in *Materials Science and Technology, A comprehensive Treatment, vol. 10 B, Nuclear Materials, part 2*, B. R. T. Frost, ed., VCH Verlagsgesellschaft mbH, Weinheim.
12. Forsyth, R. (1995) Spent nuclear fuel, A review of properties of possible relevance to corrosion processes, SKB Technical Report 95-23, Stockholm.
13. Guenther, R. J., Blahnik, D. E., Campbell, T. K., Jenquin, U. P., Mendel, J. E., Thornhill, T. K. (1989) in *Mat. Res. Soc. Proc. Vol.* **127**, W. Lutze and R. C. Ewing (eds.), 325-336.
14. Kleykamp, H. (1979) *J. Nucl. Mater.* **84**, 109-117.

15. Thomas, L. E., Einziger, R. E., and Woodley, R. E. (1989) The microstructural examination of oxidized spent PWR fuel by transmission electron microscopy, *J. Nucl. Mater*, **166**, 243-251.
16. Thomas, L. E. and Guenther, R. J. (1989) in W. Lutze and R. C. Ewing (eds), *Mat. Res. Soc. Proc. Vol.* **127**, 293-300.
17. Kleykamp, H. (1988) The chemical state of fission products in oxide fuels at different stages of the nuclear fuel cycle, *Nucl. Technology* **80**, 412-422.
18. Adachi, T., Ohnuki, M., Yoshida, N., Sonobe, T., Kawamura, W., Takkeishi, H., Gunji, K., Kimura, T., Suzuki, T., Nakahara, Y., Muromura, T., Kobayashi, Y., Okashita, H., and Yamamoto, T. (1990) *J. Nucl. Mater.***174**, 60-71.
19. Forsyth, R. S. (1990) The application of PIE techniques to the study of the corrosion of spent oxide fuel in deep-rock groundwaters, Studsvik Report NF(P)-90/43, Nyköping.
20. Kleykamp, H. (1990) *J. Nucl. Mater.***171**, 181-188.
21. Matzke, Hj., Blank, H., Coquerelle, M., Lassmann, K., Ray, I. L. F., Ronchi, C., and Walker, C. T. (1989) *J. Nucl. Mater.* **166**, 165-178.
22. Walker, C. T., Bagger, C., and Mogensen, M. (1990) Migration of fission product barium in UO_2 fuel under transient conditions, *J. Nucl. Mater.* **173**, 14-25.
23. Cordfunke, E. H. P., and Konings, R. J. M. (1988) *J. Nucl. Mater.***152**, 301-309.
24. Forsyth, R. S., and Werme, L. O. (1992) Spent fuel corrosion and dissolution, *J. Nucl. Mater.* **190**, 3-19.
25. Oversby, V. M., and Shaw, H. F. (1987) Spent fuel performance data: an analysis of data relevant to the NNWSI Project, Lawrence Livermore National Laboratory Report UCID-20926, Livermore.
26. Stroes-Gascoyne, S., Johnson, L. H., and Sellingger, D. M. (1987) *Nucl. Technol.* 77, 320-330.
27. Johnson, L. H., Stroes-Gascogne, S., Chen, J. D., Attas, D. M., Sellinger, D. M., and Delaney, H. G. (1985), The relationship between fuel element power and the leaching of ^{137}Cs and ^{129}I from irradiated UO_2 fuel in *Proc. ANS Topical Meeting Fission Product Behavior and Source Term, Snowbird, Utah, 1984*, M. F. Huebner, ed., American Nuclear Society.
28. Wilson, C. N. (1990) Results from NNWSI Series 3 spent fuel dissolution tests, Pacific Northwest Laboratories, Richland.
29. Forsyth, R. S., Jonsson, T., and Mattsson, O. (1990) Examination of reaction products on the surface of UO_2 fuel exposed to reactor coolant water during power operation, SKB Tachnical Report 90-07, SKB, Stockholm.
30. Stroes-Gascoyne, S., Johnson, L. H., Beeley, P. A., and Sellinger, D. M. (1986) Dissolution of used CANDU fuel at various temperatures and redox conditions, in L. O. Werme, ed. *Mat. Res. Soc. Proc. Vol.* **50**, 317-326.
31. Forsyth, R. S., Eklund, U-B., Mattsson, O., and Schrire, D. (1990) Examination of the surface deposit on an irradiated PWR fuel specimen subjected to corrosion in deionized water, SKB Technical Report 90-04, Stockholm.

*This work was performed under the auspices of the U.S. Department of Energy by Lawrence Livermore National Laboratory under contract No. W-7405-Eng-48.

32. Wilson, C. N. (1991) in T. A. Abrahjano and L. H. Johnson, eds., *Mat. Res. Soc. Proc. Vol.* **212**, 197-204.